

Assessment of Uranium Biokinetics and Organ Dose Estimation Following Ingestion from Groundwater in the Patiala District, Punjab, India.

Hardev Singh Virk

Department of Physics, SGGS World University, Fatehgarh Sahib-140 407, Punjab, India.

ORCID:<https://orcid.org/0000-0001-6118-610X>

Email: hardevsingh.virk@gmail.com (corresponding author)

(Received:10-07-2025; Accepted: 30-07-2025; Published Online:20-08-2025)

ABSTRACT:

Background: Uranium is a radioactive substance which is present in groundwater. Its ingestion through drinking presents both radiological and chemical risks to living organisms.

Purpose: Our purpose is to study Uranium (U) retention in human body and the radiological dose delivered to different organs and tissues causing health hazards to residents of Patiala district.

Methods: The sample collection was done in clean plastic bottles from 70 different locations of Patiala district. U estimation of groundwater was done by using the ICP-MS technique.

Results: U retention and radiological dose delivered to different organs has been estimated using Li's Model. Time dependence of U in Kidney, Liver, OST and Urinary Bladder has been studied. The maximum excretion occurs through faeces ranging from $41.89 \mu\text{g d}^{-1}$ to $371.57 \mu\text{g d}^{-1}$, followed by hair ($0.16 \mu\text{g d}^{-1}$ to $1.44 \mu\text{g d}^{-1}$), and then urine ($0.09 \mu\text{g d}^{-1}$ to $0.78 \mu\text{g d}^{-1}$).

Conclusions: The uranium concentration in groundwater of Patiala district varies from 30.10 to $267 \mu\text{g L}^{-1}$. All the recorded values of U are above the WHO recommended limits ($30 \mu\text{g L}^{-1}$). Application of Li's Model reveals that the important organs like kidneys, liver, other soft tissues and cortical bone volume are targeted by natural uranium through the ingestion route. Excretion rate of uranium from hair is higher than the urine. The highest percentage of dose is delivered to bone surfaces (38.5%), followed by kidneys (13.8%), LLI walls (11.5%), Liver (5.2%), ULI walls (4.8%), Red marrow (4.1%), and other organs and tissues (1.3%).

Keywords: Uranium, Groundwater, Biokinetic modelling, Uranium Retention, Health Hazards

1. Introduction and Review of Literature

As per UNESCO World Water Report of 2022, Bangladesh, China, India, Indonesia, Iran, Pakistan, and Turkey emerge as prominent groundwater extractors in the Asia-Pacific region, collectively contributing to around 60% of global groundwater withdrawal [1]. This groundwater serves as a vital resource for sustaining ecosystems and fulfilling the potable water requirements of millions of people worldwide. However, the escalating contamination of groundwater presents a significant challenge, with various pollutants such as radionuclides and heavy metals infiltrating it from

diverse sources, including industrial activities, agriculture, leaching, nuclear facilities, and geological processes [2, 3, 4]. Once deposited on the ground, radionuclides can permeate soil, aquatic environments, and vegetation, posing risks to entire ecosystems. Emitting radiation during decay, radionuclides have the potential to migrate through soil and penetrate aquifers, posing serious threats to human health and ecological equilibrium. The interaction between radionuclides and groundwater reservoirs has become a focal point of concern, prompting extensive research in the field of environmental science globally [5, 6, 7, 8, 9]. Several studies have been conducted to elucidate the transport

mechanisms and fate of radionuclides within ground-water systems, aiming to predict potential sources of contamination [10, 11, 12, 13]. Uranium, distinguished among radionuclides, presents dual radiological and chemical toxicity risks to human health, making it a focal point of current research efforts. Human exposure to uranium can manifest through various pathways, including water, food, and air, with drinking water representing the primary and most substantial route of intake [14]. Natural water sources frequently exhibit a concentration ratio of $^{234}\text{U}/^{238}\text{U}$ greater than 1. The transfer of ^{234}U from sediment to water is facilitated by the energetic conversion of ^{238}U to ^{234}U through α -emission processes [15]. The different isotopes within the uranium decay series interact among soil, plants, and water to enable them to dissolve and migrate toward plants, subsequently entering the food chain [16]. Once incorporated into the food chain, radionuclides may accumulate in organisms at higher trophic levels, posing potential health risks to both humans and wildlife. Such contamination can persist for extended durations, as certain radionuclides possess half-lives spanning thousands of years, rendering them radioactive for significant periods. Uranium's dual attributes of radiation emission and toxic properties pose significant concerns regarding human health. Its presence in groundwater sources can result in severe health implications, including cellular and DNA damage, as well as various illnesses such as stomach and urinary organ cancers, leukemia, kidney infections, and lung infections, as evidenced by multiple studies [17, 18, 19, 20]. This study aimed to investigate the specific regions within the human body affected by natural uranium-contaminated water resources in the Patiala district of Punjab, India, employing the Li's Uranium Hair Compartment Biokinetic Model [21]. The Biokinetic Model provides a structured framework for comprehending the migration, retention, and distribution of uranium within various organs. Additionally, this research endeavors to explore the time-dependent dynamics of uranium within the human body. The purpose of this study is to investigate the retention of the uranium in all compartments of human body

in addition to urinary, faecal, and hair excretion after ingestion of water. Risk due to consumption of drinking water having high uranium concentration in groundwater in Punjab State of India has been reported [22]. These systematic investigations can facilitate the prediction of radionuclide behavior and the identification of potential areas of concern, thereby aiding in the development of effective remediation strategies.

2. Objectives of Study, its Scope and Limitations

Our objective is to study Uranium concentration in groundwater collected from different locations of Patiala district to investigate the health hazards to residents living in the area of our study. Our next purpose is to investigate the uranium retention, excretion and radiological dose delivered due to ingestion of uranium by the application of Li's Uranium Hair Compartment Biokinetic Model in Patiala district for the first time. The reports of International Commission on Radiological Protection (ICRP) provide the biokinetic model for different radionuclides including uranium. Li's Uranium Hair Compartment Biokinetic Model proposed hair as the one of the routes of excretion. Our purpose is to study its advantages in comparison to ICRP model.

The scope of our study is to investigate variation of Uranium concentration in groundwater of Patiala district, estimate the health hazards to residents of the study area, and apply it to groundwater of other 25 districts of Punjab state. However, there is one limitation that it is an empirical study based on Li's model and needs to be repeated after every year due to variation in quality of groundwater caused by rainfall and local geology.

3. Methodology and Materials

3.1. Study Location

Fig. 1 represents 70 locations within the Patiala district, Punjab (India), which lies between $29^{\circ} 49'$ to $30^{\circ} 40'$ north latitudes and $75^{\circ} 58'$ to $76^{\circ} 48'$ east longitudes. Total geographical area of the district is 3218 sq. km. The Patiala district is divided into six subdivisions (tehsils) namely Patiala, Nabha, Patran, Ghanaur,

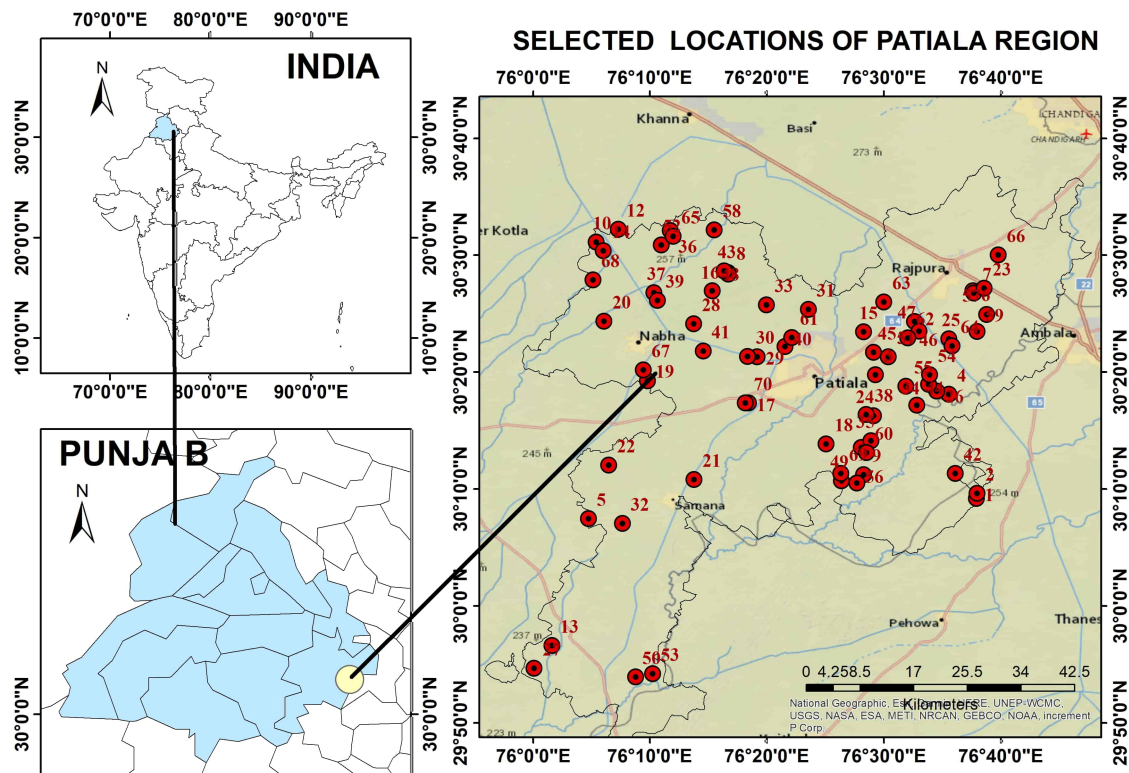


Figure 1: Study locations of Patiala District Patiala

Rajpura and Samana comprising eight-community development blocks for the purpose of administration. Uranium distribution in S-E part of district (Samana and Patran tehsils) is somewhat skewed. A comprehensive analysis of spatial distribution warrants future investigation, with heightened emphasis on collecting maximum samples from diverse districts within Punjab. This study also emphasizes the continuous need for vigilance and measures to mitigate the potential adverse effects of uranium on human health. It is evident that urgent action is required to address this pressing issue and safeguard the well-being of the inhabitants of Patiala district.

3.2. Ground Water Quality

The district is occupied by Indo-Gangetic alluvial plain of Quaternary age and falls in Ghaggar basin. The ground water occurs in alluvium formations comprising fine to coarse sand, which forms the potential aquifers. In the shallow aquifer (up to 50m) ground water occurs under unconfined/water table conditions, whereas in deeper aquifer, semi-confined/confined conditions exist. The traditional dug wells tapping the shallow aquifer are not in use and most of them have

been abandoned; however, this aquifer is being tapped by the hand pumps and shallow tube wells, which are widely used for domestic purposes. The Central Ground Water Board (CGWB) has carried out studies [23] for chemical quality of ground water in the area. The ground water of the district is alkaline in nature. The electrical conductivity (EC) in the area ranges from 687 to 4100 micromhos/cm. Nitrate values range between 11.50–2553 mg/l and fluoride concentration ranges from 1.5 to 9.2 mg/l and observed beyond the safe limits suggested by the WHO, thus the ground water is harmful for human consumption in Patiala district with 98% of the sampling locations having fluoride levels higher than the permissible limit [24, 25]. Virk [26] classified Patiala district as a “Hot Spot” due to poor quality of its groundwater having highest values of sulphate, nitrate and fluoride contents in Punjab. Surprisingly, groundwater fluoride distribution in Patiala district follows a similar pattern as found for U distribution [25].

3.3. Sample Collection

Water samples were collected in 500 ml amber coloured superior quality plastic bottles from the area of study

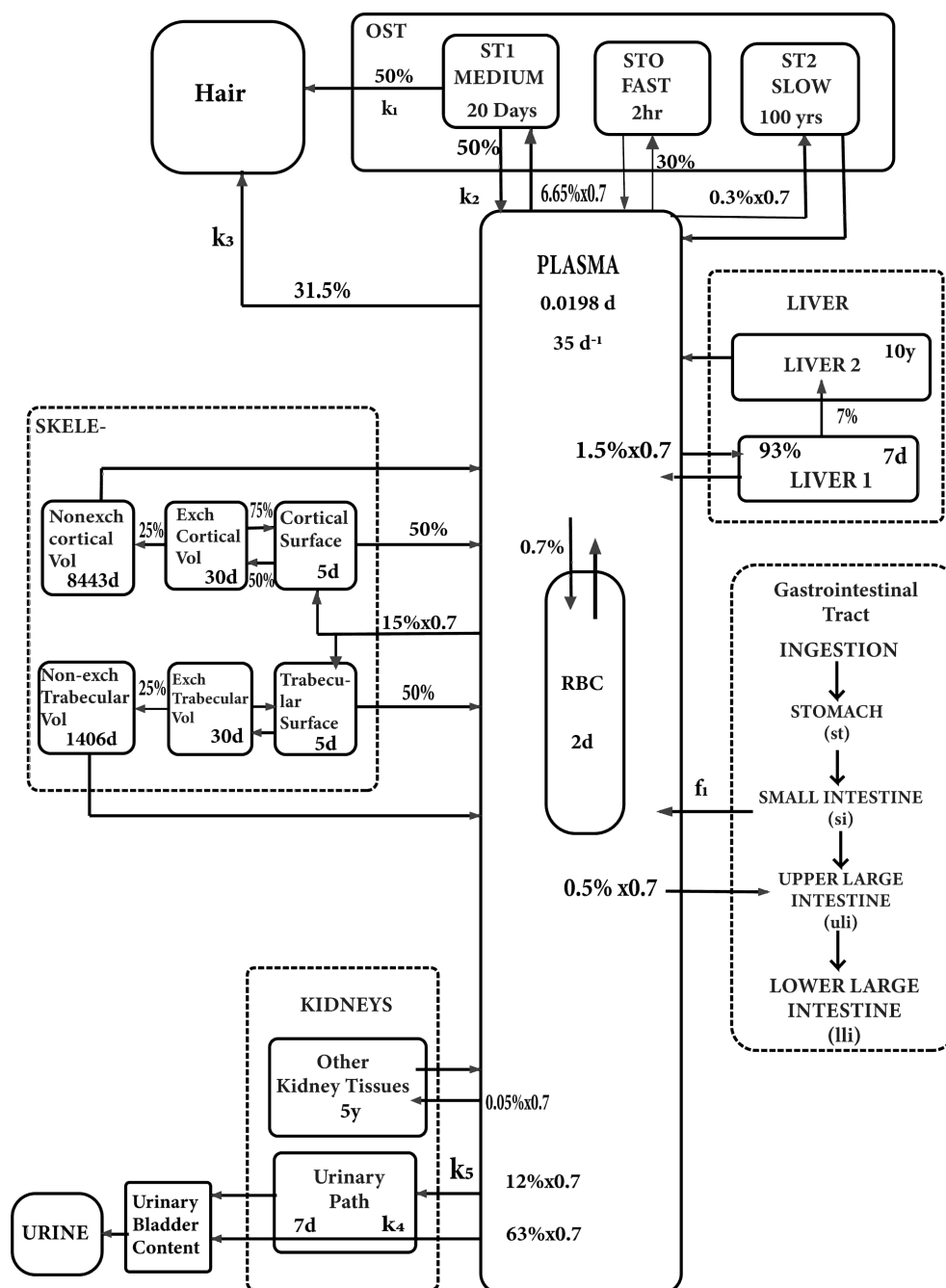


Figure 2: Hair Biokinetic model (Li et al. 2009)

by the field staff of Department of Water Supply and Sanitation (DWSS) under the World Bank Project sanctioned to Government of Punjab [27]. The cleaning of bottles was carried out by washing first with soap solution and then with distilled water. Next step was rinsing the bottles with deionised water and drying with a blower. Groundwater from the source was allowed to flow freely for 5–10 minutes before collection in plastic bottles. Samples were subject to filtration using the 0.2-micron filters on the spot. 2 ml of conc. HNO₃ was added to each sample and labelled using

scotch tape. Nitric acid solubilization is required before the determination of total recoverable uranium. The preservation and digestion of uranium in acid is used to aid breakdown of complexes and to minimize interferences by poly-atoms.

3.4. Sample Analysis

The methodology for sample analysis has been described in detail by Virk [28]. The uranium analysis of collected water samples has been done using Model 7700 Agilent Series ICP-MS following standard procedure in the Regional Advanced Water Testing

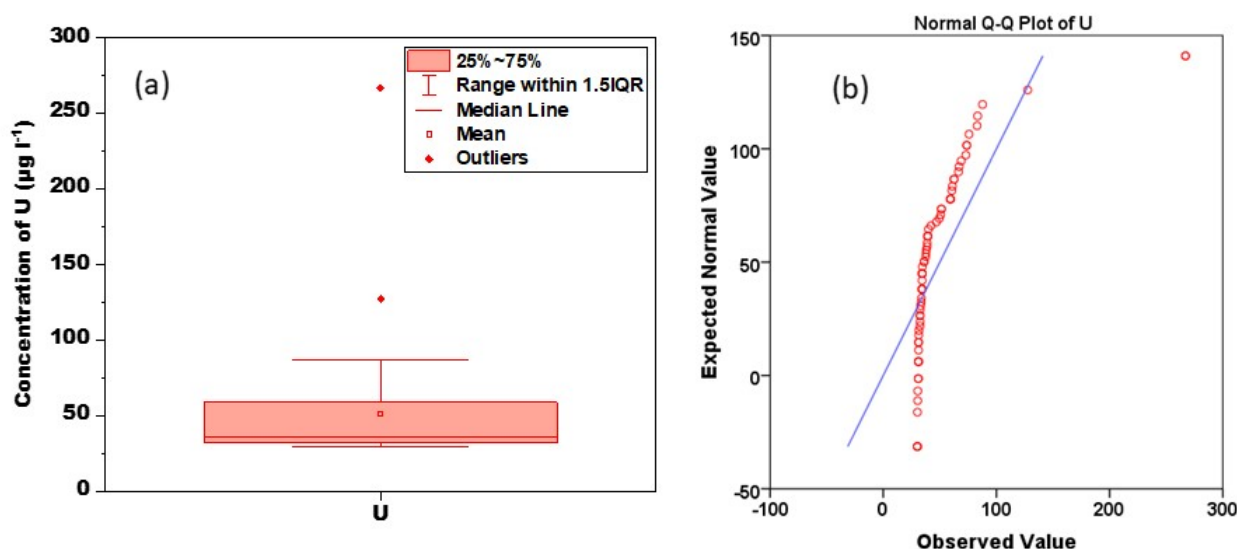


Figure 3: (a) Box plot and (b) QQ plot

Laboratory (RAWTL) in SAS Nagar (Mohali), Punjab, India. The method measures ions produced by a radiofrequency inductively coupled plasma (ICP). Analyte species originating in a liquid are nebulized and the resulting aerosol is transported by Argon gas into the plasma torch. The ions produced by high temperatures are entrained in the plasma gas and introduced, by means of an interface, into a mass spectrometer. The ions produced in the plasma are sorted according to their mass-to-charge ratios and quantified with a channel electron multiplier. Interferences must be assessed, and valid corrections applied. Interference correction must include compensation for background ions contributed by the plasma gas, reagents, and constituents of the sample matrix. Data analysis is done automatically by inbuilt system of ICP-MS. In addition to Uranium, data for 40 more trace elements can be retrieved using ICP-MS.

3.5. Calibration of ICP-MS

Calibration experiment is necessary for the estimation of concentration of heavy metals in . using the Agilent 7700 Series ICP-MS, with a detection limit ranging from <100 ppb to <1 ppt. The quantification was performed against the Certified Reference Material (CRM) 2A by Agilent Technologies (Part Number 8500-6940).

Six concentration standards were meticulously prepared and introduced into the ICP-MS through an S10 auto-sampler unit. To establish a reliable calibration, a linear curve was constructed, exhibiting a high correlation coefficient ($R^2 \geq 0.999$) for all selected metals. Following the calibration, one quality control (QC) check and analysis of two different standards (20 and 50 ppb) were conducted both before and after sample processing. The Relative Standard Deviation (RSD) was determined to be below 4%, aligning with the standards set by the Bureau of Indian Standards (BIS) for measuring drinking water samples. This comprehensive methodology ensures the accuracy and precision of Uranium concentration measurements, supported by rigorous calibration procedures and quality control checks in accordance with industry standards [29].

4. Application of Li's Uranium Hair Compartment Biokinetic Model

An earlier version of Li's Biokinetic Model of Uranium specifically focuses on the time-dependent processes of retention, distribution and elimination of the radionuclides within the human body [18]. Fig. 2 serves as a comprehensive schematic representation of the Li's Uranium Hair Compartment Biokinetic Model [21], delineating the intricate pathways of uranium and its migration within the biological system.

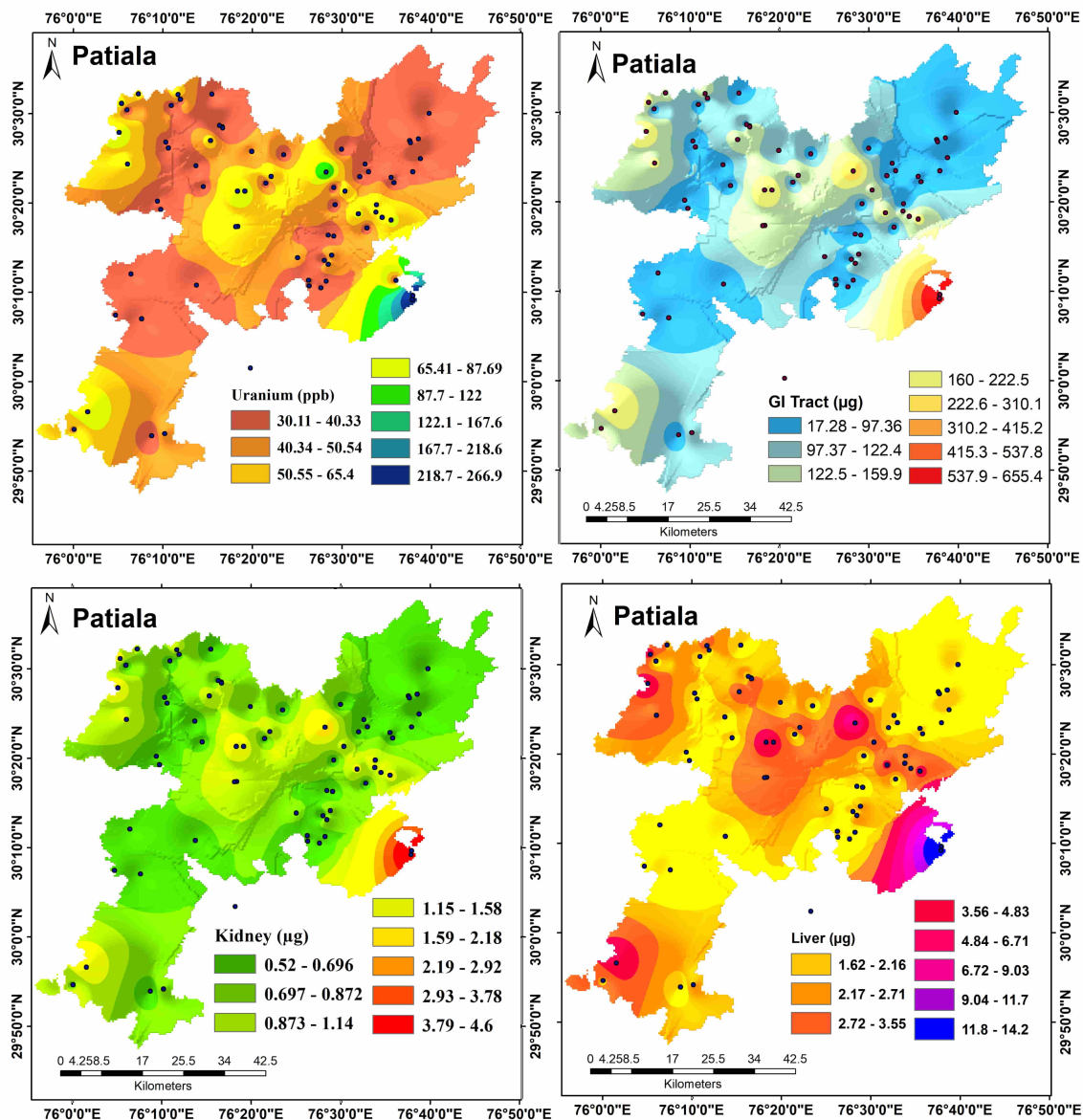


Figure 4: Spatial distribution of uranium concentration and its retention in GIT, kidneys and Liver compartments

In biokinetic model, the ingestion pathway commences within the gastrointestinal tract (GIT), wherein uranium is absorbed primarily through the small intestine. Subsequently, it enters the bloodstream, facilitating its distribution to various organs and tissues across the entirety of the body. The biokinetic model adopts a compartmental framework, partitioning the body's organs and tissues into discrete compartments that engage in interactions and activity exchange. Each compartment exhibits uniform kinetic properties. Through this compartmentalized approach, the model dissects the intricate interplay among various compartments,

furnishing invaluable insights into the overarching behaviour of uranium within the body [30]. The transfer rates delineated in the figure 2 serve to elucidate the dynamics of radionuclide transportation among compartments within the adult public. According to the specified model, within the hair model framework, uranium is conveyed to the bloodstream via the small intestine at a rate denoted by f_1 . Following this, 30% of the activity is translocated from the bloodstream to STO, while the remaining 70% is disseminated among all other compartments. The 52.5% of the uranium content in the bloodstream is subsequently transferred to urine, facilitated by either the urinary pathway

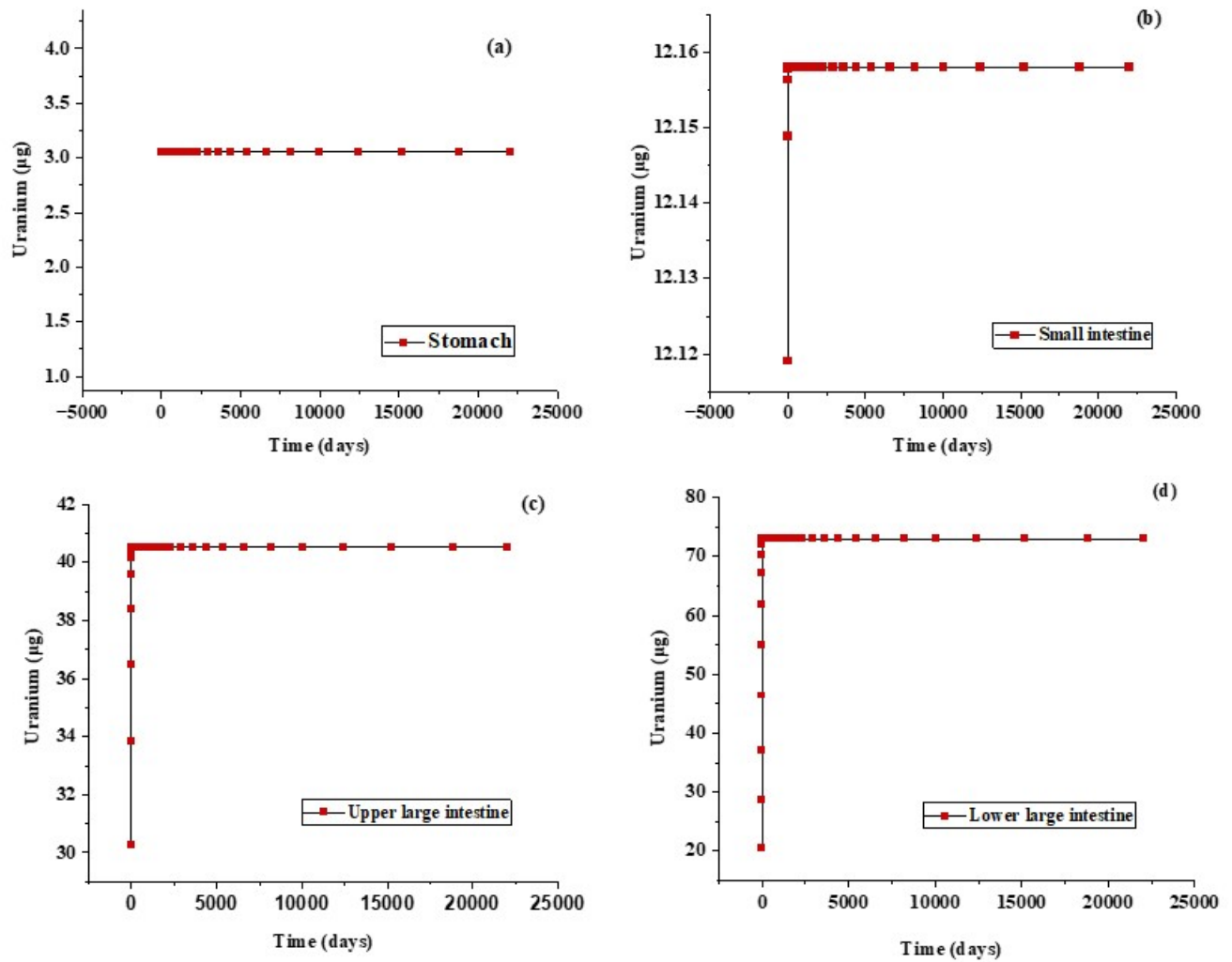


Figure 5: Time dependence studies of uranium in Gastrointestinal Tract System (GIT)

or the urinary bladder [21]. The hair compartmental biokinetic model proposed hair as the one of the routes of excretion, in which uranium is absorbed into the bloodstream, before being transferred to the OST compartment and eventually excreted

through the hair; this is the first excretion route from hair with the first order kinetics. While the second route is assumed to be direct transfer of uranium from the blood to hair with third order kinetics.

$$\frac{dq_{i,n}(t)}{dt} = I_{i,n}(t) + \sum_{\substack{j=1 \\ j \neq i}}^N q_{j,n}(t)k_{i,j,n} - q_{i,n}(t) \sum_{\substack{j=1 \\ j \neq i}}^N (k_{i,j,n} + \lambda_n) + \sum_{m=1}^{n-1} q_{i,m}(t)\beta_{n,m}\lambda_n \quad (1)$$

Where $I_{i,n}(t)$, $k_{i,j,n}$, $q_{i,n}(t)$, λ_n , and $\beta_{n,m}$ are known as the compartmental input flow rate, transfer rate from one compartment to another, number of transactions, nuclide ingrowth atoms at time t in

compartment i , radionuclide decay constant λ , and branching fraction β , respectively.

The equation (1) represents the retention of uranium in the different organs and tissues including, kidney, liver,

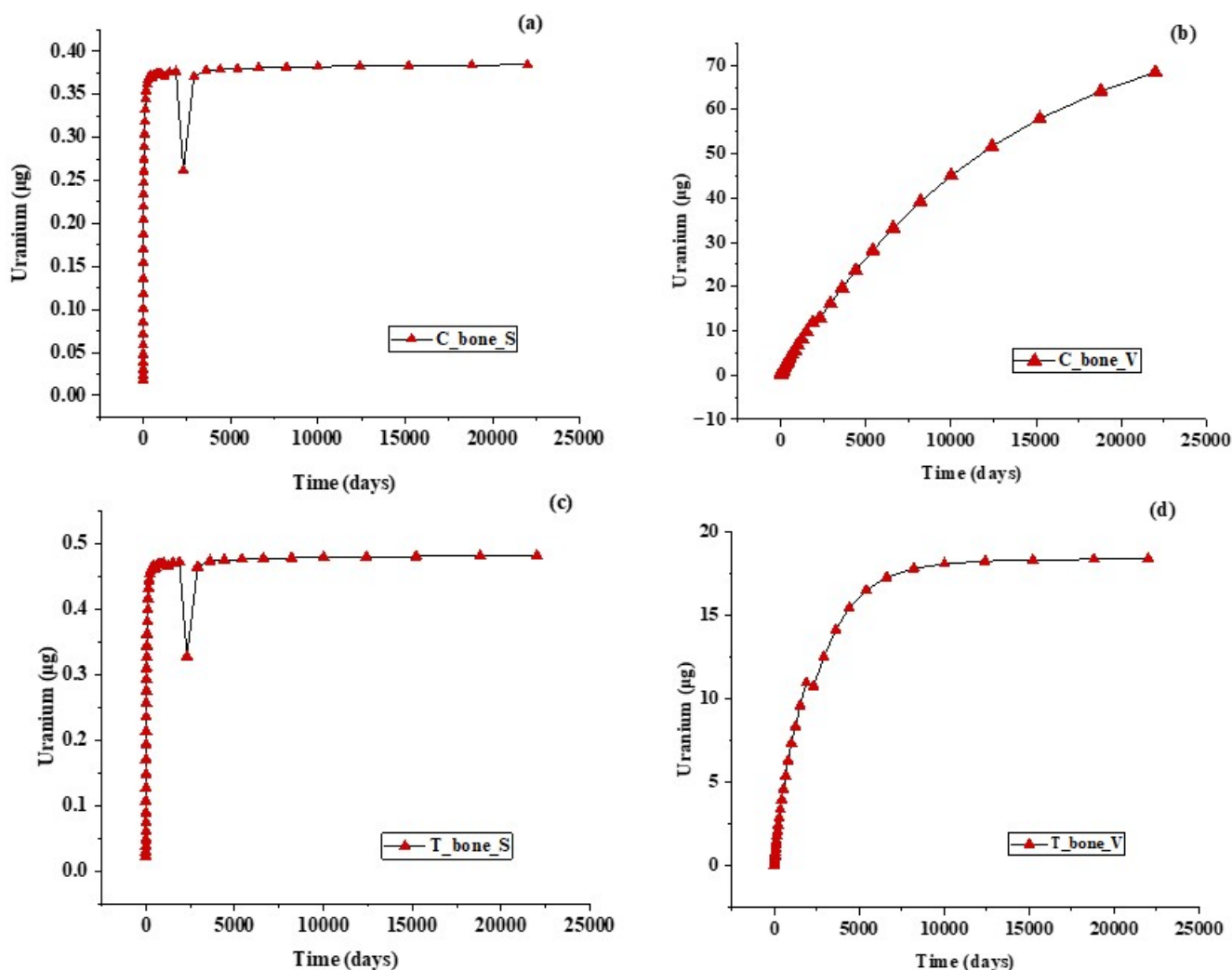


Figure 6: Time dependence studies of uranium in Skeleton

soft tissues, etc. for the hair compartment biokinetic model [21] There have been several investigations into uranium ingestion in drinking water that use biokinetic models to justify the behavior of uranium within the human body [31, 32, 33, 34, 35]. Where $I_{i,n}(t)$, $k_{i,j,n}$, $q_{i,n}(t)$, λ_n , $\beta_{n,m}$ are known as Compartmental input flow rate, transfer rate from one compartment to other, n number of transactions, nuclide ingrowths atoms at time t in compartment i , λ , radionuclides decay constant and β , branching fraction, respectively. The advantage of Li's Hair Biokinetic Model [21] over ICRP Biokinetic Model [36, 37] is that determination of the uranium in hair may yield better insights for internal dosimetry even a long time after an exposure incident. The model is applicable for chronic exposure

as well as for an acute exposure incident. In the latter case, the hair sample can be collected and analyzed even several days after the incident, whereas urinalysis requires sample collection shortly after the exposure. This new model is also used to predict uranium excretion in human hair as a bioassay indicator due to elevated uranium intakes.

5. Analysis and Interpretation of Data

A comprehensive investigation was undertaken within the Patiala district of Punjab, India, with the aim of assessing the uranium concentration levels across various drinking water sources.

Table 1 presents the uranium concentration in groundwater at 70 locations of Patiala district, and retention

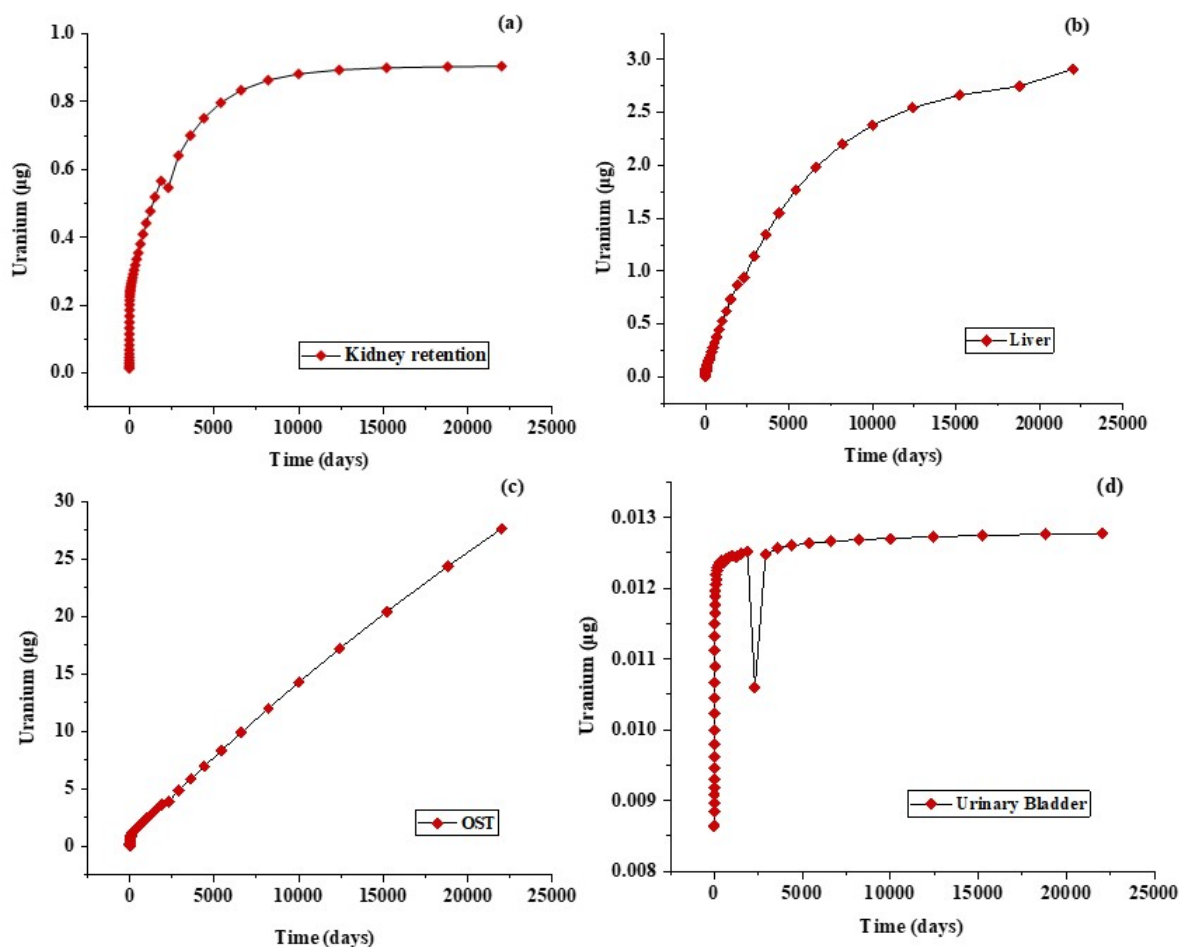


Figure 7: Time dependence of uranium in (a) Kidney, (b) Liver, (c) OST and (d) Urinary Bladder

levels in various organs and tissues of human body. The estimated uranium concentrations ranged from $30.10 \mu\text{g L}^{-1}$ to $267 \mu\text{g L}^{-1}$, as per the variation shown in the Fig. 3a and Table 1. Fig. 3a illustrated few outliers with potentially higher uranium concentration in Ahru Kalan and Ahru Khurd villages of Patiala district. Fig. 3b demonstrates the non-normal distribution of uranium concentration in the studied area and the results are in accordance with the similar behaviour of radionuclides, heavy metals and other pollutants in different types of vicinities [2, 38, 39, 40]. Fig. 4 illustrates the spatial variability of uranium distribution across distinct geographical locales, highlighting a non-uniform dispersion pattern of this radionuclide within these areas. This study delves into the pathway of uranium ingestion, particularly focusing on the implications of sustained exposure over a continuous duration of 60 years.

5.1. Gastrointestinal Tract (GIT)

Ingestion is the main pathway of the exposure of the natural radionuclides in water to the general population and GIT is the path through which the ingested uranium enters the bloodstream. High concentration of the uranium may lead to high retention of uranium in different body organs. Within the gastrointestinal tract (GIT) region, the average retention of uranium is recorded at $126.83 \mu\text{g}$, encompassing a range of individual values spanning from 14.58 to $655.50 \mu\text{g}$, as detailed in Table 1. The uranium retention in stomach (ST), small intestine (SI), upper large intestine (ULI), and lower large intestine varied from $1.76 \mu\text{g}$ to $15.58 \mu\text{g}$, $6.98 \mu\text{g}$ to $61.93 \mu\text{g}$, $23.27 \mu\text{g}$ to $206.43 \mu\text{g}$ and $41.89 \mu\text{g}$ to $371.57 \mu\text{g}$, respectively, and their spatial distribution is depicted in Fig. 4. The small intestine functions as the principal conduit for uranium absorption into the bloodstream,

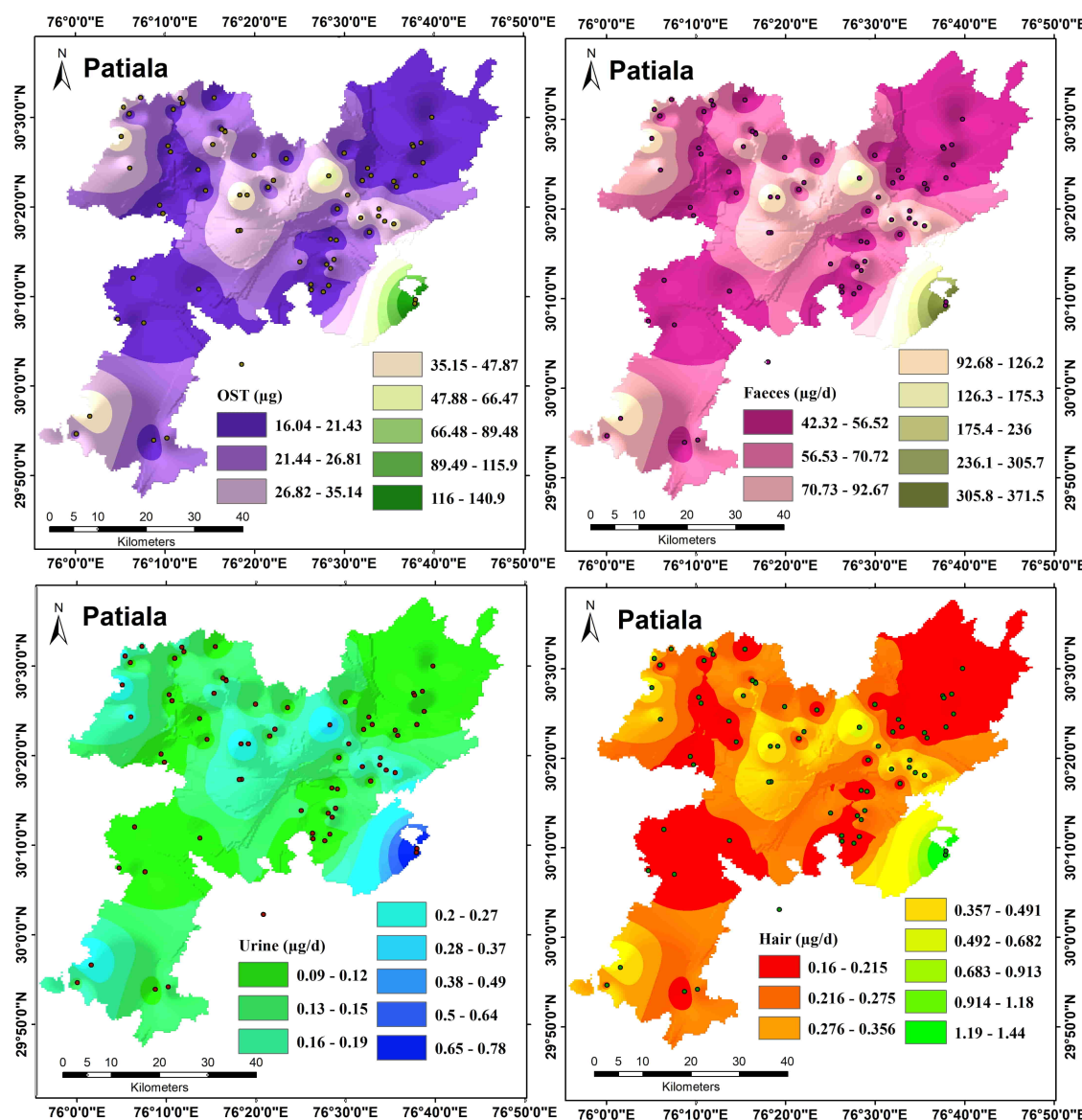


Figure 8: Spatial distribution of uranium retention in OST and uranium excretion in Faeces, Urine and Hair compartments

thereby facilitating systemic exposure to its radioactive properties throughout the entire body. The time dependence studies of uranium concentration demonstrate the early saturation in gastrointestinal tract (Fig. 5).

5.2. Blood

Following ingestion, uranium swiftly enters the blood-stream, as evidenced in the previous studies and those investigations have consistently indicated a significant portion of the ingested uranium becomes associated with red blood cells [41, 42]. Upon entering the blood-stream, uranium is either assimilated by tissues or eliminated through urinary excretion. Uranium associated with red blood cells (RBCs) reverts its activity to

plasma within a span of 2 days (Fig.2). In this context, the mean retention of uranium was determined to be 0.045 µg, with individual values spanning from 0.020 to 0.26 µg (Table 1).

5.3. Skeleton

Within bones, the behaviour of uranyl ions parallels that of calcium ions. Uranyl ions undergo exchange with calcium ions at bone surfaces. However, these ions do not actively participate in crystal formation or diffuse into the bone mineral crystals. The rapidly exchangeable activity within bones primarily resides on the bone surfaces, whereas the slowly exchangeable activity is distributed within the volume of the bones.

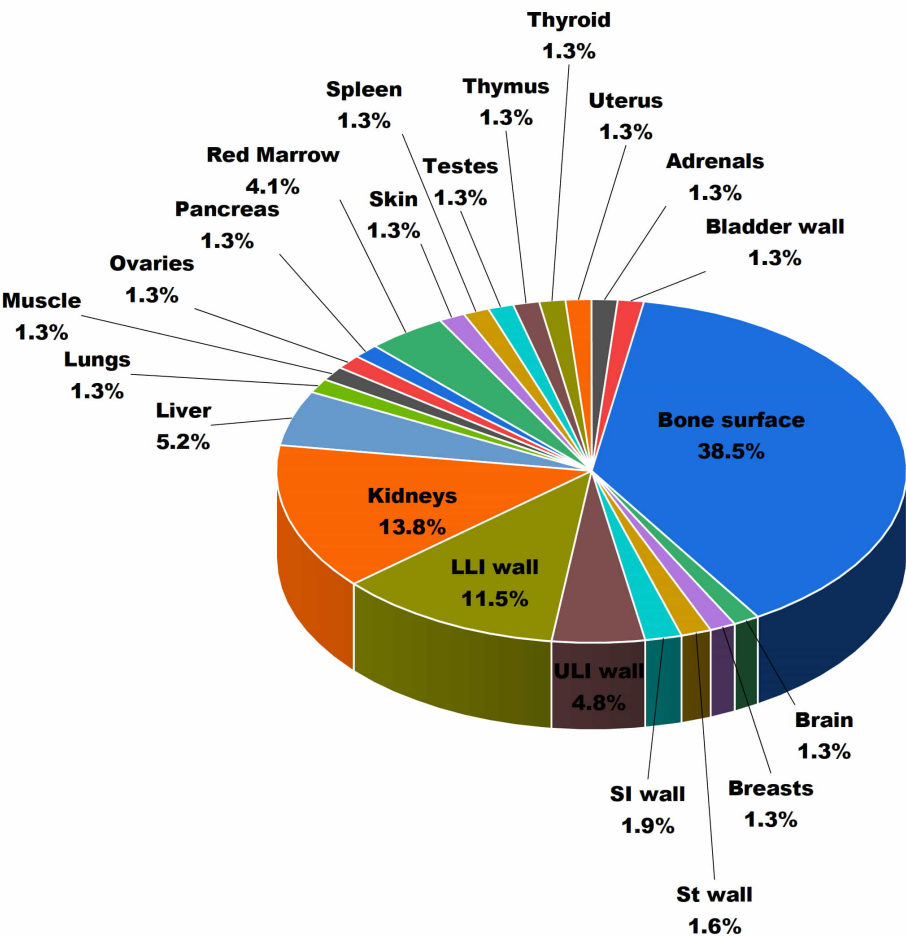


Figure 9: Pie chart showing distribution of doses to different organs or tissues in human body

This bone volume undergoes exchange primarily with the bone surface rather than with plasma [43]. Skeleton compartment is divided into four primary parts: cortical bone surface (C_bone_S), cortical bone volume (C_bone_V), trabecular bone surface (T_bone_S), and trabecular bone volume (T_bone_V) with mean uranium retention of 0.38 μg (0.22-1.96 μg), 68.39 μg (39.27-348.30 μg), 0.48 μg (0.28-2.45 μg), and 18.37 μg (10.55-93.57 μg), respectively (Table 1). With the sole exception of C_bone_V, the various compartments of the skeletal structure, encompassing C_bone_S, T_bone_S, and T_bone_V, demonstrate indications of saturation subsequent to a brief, uninterrupted exposure to uranium through ingestion via drinking water as shown in the time dependence studies (Fig. 6)

5.4. Kidneys

The kidney compartment comprises two distinct subdivisions: other kidney tissues and the urinary pathway. Uranium ingress into the kidney through other soft tissues yields a removal half-life of approximately 5 years, consequently leading to elevated activity levels within the kidneys. For kidneys, the average retention of uranium is quantified at 0.90 μg , with individual values ranging from 0.52 to 4.60 μg , as illustrated in spatial distribution maps (Fig. 4) and Table 1. As delineated in Fig. 7a, saturation of uranium within the kidney is observed to transpire following approximately 35 years of exposure, thereby underscoring the potential for chemical risks at this anatomical site.

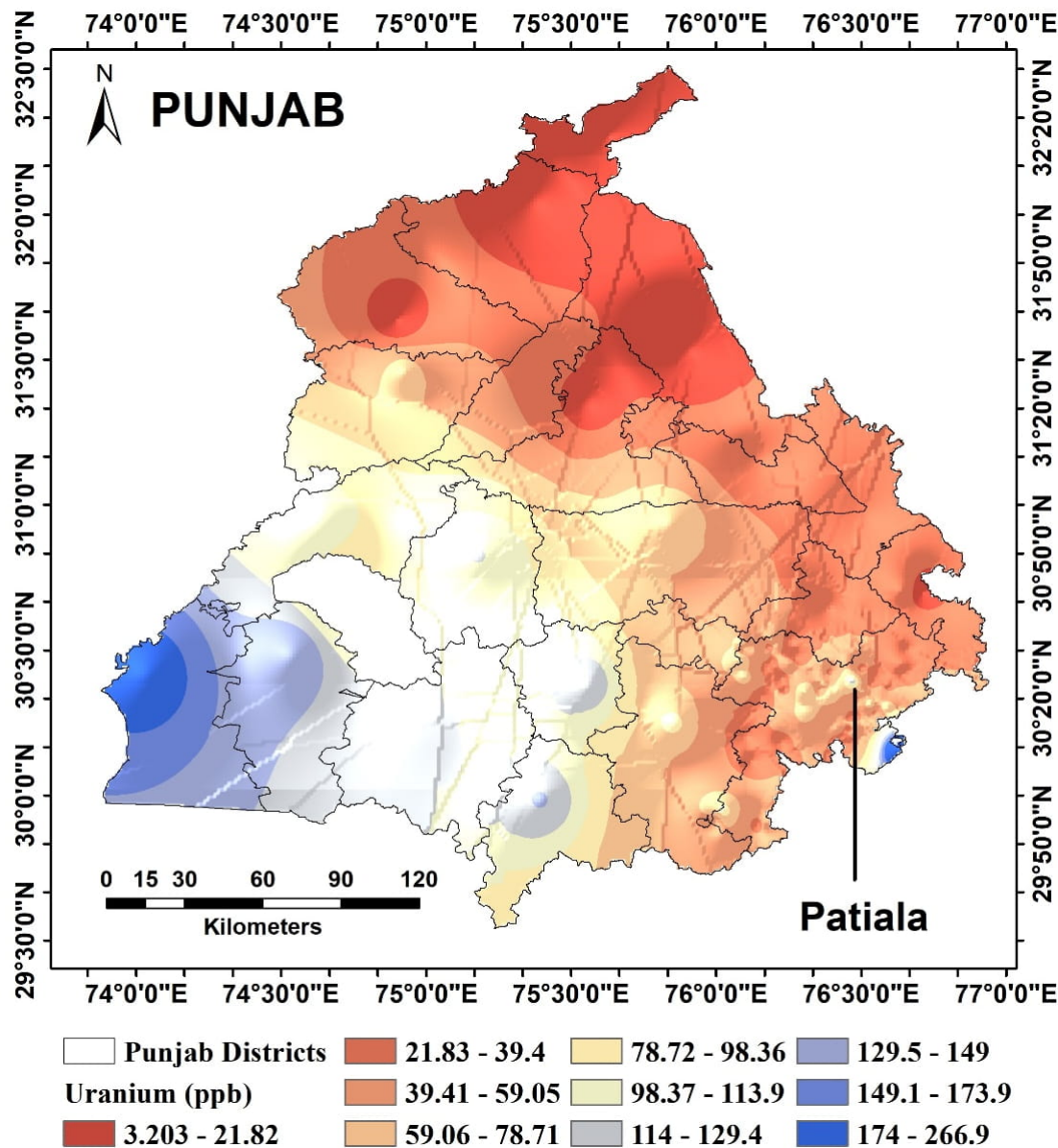


Figure 10: Uranium distribution in Punjab Province

5.5. Liver

The liver compartment is segmented into two distinct regions: liver 1 and liver 2. Uranium ingress into this compartment primarily occurs through the liver 1 site, where approximately 93% of the uranium returns to the bloodstream. A residual 7% of the uranium proceeds to the liver specifically liver 2, where the activity undergoes reintegration into the bloodstream over a 10-year period at this site. The mean retention of uranium within the liver compartment is determined to be 2.79 μg (Fig. 4). Time-dependent studies have illustrated the non-saturation behaviour of uranium in the liver (Fig. 7b).

5.6. Other soft tissues (OST)

The average uranium retention in these tissues (OST) was observed to be 27.67 μg , with values ranging from 15.86 to 140.91 μg (Fig. 8) as given in Table 1. The duration of uranium residence within each compartment is partially regulated by their respective removal half-times. Specifically, for ST0, ST1, and ST2 compartments, the removal half-times were observed to be 2 hours, 20 days, and 100 years, respectively, as depicted in the biokinetic model (Fig. 2). Consequently, owing to the slow turnover rate associated with ST2, temporal dependency studies have unveiled a non-saturation phenomenon within this site even after 60 years (Fig. 7c).

Table 1: Uranium retention in various organs and tissues

Sr. No.	Locations	Uranium Conc. (µg L ⁻¹)	GI tract	blood	Skeleton				Kidneys		Liver ₁ + Liver ₂ (µg)	OST (ST1 +ST0 +ST2) (µg g ⁻¹)	Urinary Bladder (µg)	Whole Body (µg)	Excretion		
					C_bone_S	C_bone_V	T_bone_S	T_bone_V	R*	C+					Faeces (µg d ⁻¹)	Urine (µg d ⁻¹)	Hair (µg d ⁻¹)
			ST +SI +ULI +LLI (µg)	Plasma + RBC (µg)													
1	Ahru Kalan	267	655.5	0.18	1.96	348.3	2.45	93.57	4.6	0.0148	14.22	140.91	0.065	1261.75	371.57	0.78	1.44
2	Ahru Khurd	267	655.5	0.18	1.96	348.3	2.45	93.57	4.6	0.0148	14.22	140.91	0.065	1261.75	371.57	0.78	1.44
3	Assarpur	33	81.02	0.022	0.24	43.05	0.3	11.57	0.57	0.0018	1.76	17.42	0.008	155.95	45.92	0.1	0.18
4	Asse Majra	73.76	181.09	0.049	0.54	96.22	0.68	25.85	1.27	0.0041	3.93	38.93	0.018	348.56	102.65	0.22	0.4
5	Balamgarh	38.77	95.18	0.026	0.28	50.58	0.36	13.59	0.67	0.0022	2.06	20.46	0.0094	183.21	53.95	0.11	0.21
6	Bathonia Kalan	39.3	96.48	0.261	0.29	51.27	0.36	13.77	0.68	0.0022	2.09	20.74	0.0096	185.72	54.69	0.11	0.21
7	Bathonia Khurd	39.3	96.48	0.261	0.29	51.27	0.36	13.77	0.68	0.0022	2.09	20.74	0.0096	185.72	54.69	0.11	0.21
8	Bazidri	30.1	73.9	0.02	0.22	39.27	0.28	10.55	0.52	0.0017	1.6	15.88	0.0073	142.24	41.89	0.09	0.16
9	Bhuner Heri	37.55	92.19	0.025	0.28	48.98	0.34	13.16	0.65	0.0021	2	19.82	0.0092	177.45	52.26	0.11	0.2
10	Birdhno	75.8	186.09	0.05	0.56	98.88	0.7	26.56	1.31	0.0042	4.04	40	0.0185	358.2	105.49	0.22	0.41
11	Budanpur	31	76.11	0.021	0.23	40.44	0.29	10.86	0.53	0.0017	1.65	16.36	0.0076	146.49	43.14	0.09	0.17
12	Bugga Khurd	50.75	124.59	0.034	0.37	66.2	0.47	17.79	0.87	0.0028	2.7	26.78	0.0124	239.83	70.63	0.15	0.27
13	Chunagra	87.76	215.46	0.058	0.64	114.48	0.81	30.76	1.51	0.0049	4.67	46.31	0.0214	414.72	122.13	0.26	0.47
14	Dandrala Dhindsa	30.2	74.14	0.02	0.22	39.4	0.28	10.58	0.52	0.0017	1.61	15.94	0.0074	142.71	42.03	0.09	0.16
15	Daun Kalan	127.6	313.26	0.085	0.94	166.45	1.17	44.72	2.2	0.0071	6.79	67.34	0.0311	602.99	177.57	0.37	0.69
16	Barhe	82.93	203.6	0.055	0.61	108.18	0.76	29.06	1.43	0.0046	4.42	43.77	0.0202	391.9	115.41	0.24	0.45
17	Dera Saini Majra	62.5	153.44	0.042	0.46	81.53	0.57	21.9	1.08	0.0035	3.33	32.98	0.0152	295.35	86.98	0.18	0.34
18	Dera Shingara Singh	42.2	103.6	0.028	0.31	55.05	0.39	14.79	0.73	0.0023	2.25	22.27	0.0103	199.42	58.73	0.12	0.23

19	Dharoki	31.1	76.35	0.021	0.23	40.57	0.29	10.9	0.54	0.0017	1.66	16.41	0.0076	146.97	43.28	0.09	0.17
20	Dhingi	67.04	164.59	0.045	0.49	87.45	0.62	23.49	1.16	0.0037	3.57	35.38	0.0163	316.81	93.3	0.2	0.36
21	Fatehpur	32.67	80.21	0.022	0.24	42.62	0.3	11.45	0.56	0.0018	1.74	17.24	0.008	154.39	45.47	0.1	0.18
22	Gajewas	30.4	74.63	0.02	0.22	39.66	0.28	10.65	0.52	0.0017	1.62	16.04	0.0074	143.66	42.31	0.09	0.16
23	Gandian	39.3	96.48	0.261	0.29	51.27	0.36	13.77	0.68	0.0022	2.09	20.74	0.0096	185.72	54.69	0.11	0.21
24	Ghanour	34.39	84.43	0.023	0.25	44.86	0.32	12.05	0.59	0.0019	1.83	18.15	0.0084	162.51	47.86	0.1	0.19
25	Ghungrana	38.8	95.26	0.026	0.28	50.61	0.36	13.6	0.67	0.0022	2.07	20.48	0.0095	183.35	54	0.11	0.21
26	Haripur Jhugian	59.3	145.58	0.039	0.43	77.36	0.54	20.78	1.02	0.0033	3.16	31.29	0.0145	280.23	82.52	0.17	0.32
27	Hariyou Khurd	49.5	121.53	0.033	0.36	64.57	0.45	17.35	0.85	0.0028	2.64	26.12	0.0121	233.92	68.89	0.14	0.27
28	Hiana Khurd	31.2	76.6	0.021	0.23	40.7	0.29	10.93	0.54	0.0017	1.66	16.47	0.0076	147.44	43.42	0.09	0.17
29	Inderpura	73.76	181.08	0.049	0.54	96.22	0.68	25.85	1.27	0.0041	3.93	38.93	0.018	348.56	102.65	0.22	0.4
30	Kalyan	82.93	203.6	0.055	0.61	108.18	0.76	29.06	1.43	0.0046	4.42	43.77	0.0202	391.9	115.41	0.25	0.45
31	Kassiana	34.3	84.21	0.023	0.25	44.74	0.31	12.02	0.59	0.002	1.83	18.1	0.0084	162.09	47.73	0.1	0.18
32	Dharamgarh	31.21	76.62	0.021	0.23	40.71	0.29	10.94	0.54	0.0017	1.66	16.47	0.0076	147.49	43.43	0.09	0.17
33	Kath Mathi	39.94	98.05	0.027	0.29	52.1	0.37	14	0.69	0.0022	2.13	21.08	0.0097	188.74	55.58	0.12	0.22
34	Katlahar	59.3	145.58	0.039	0.43	77.36	0.54	20.78	1.02	0.0033	3.16	31.29	0.0145	280.23	82.52	0.17	0.32
35	Khaktan Khurd	51.33	126.02	0.034	0.38	66.96	0.47	17.99	0.88	0.0028	2.73	27.09	0.0125	242.57	77.43	0.15	0.28
36	Khanora	68.81	168.93	0.046	0.5	89.76	0.63	24.11	1.19	0.0038	3.66	36.31	0.0168	325.17	95.76	0.2	0.37
37	Khokh	36.1	88.63	0.024	0.27	47.09	0.33	12.65	0.62	0.002	1.92	19.05	0.0088	170.6	50.24	0.11	0.19
38	Khuda	34.39	84.43	0.023	0.25	44.86	0.32	12.05	0.59	0.0019	1.83	18.15	0.0084	162.51	47.86	0.1	0.19
39	Kotli	36.1	88.63	0.024	0.27	47.09	0.33	12.65	0.62	0.002	1.92	19.05	0.0088	170.6	50.24	0.11	0.19
40	Lachkani	32.52	79.84	0.022	0.24	42.42	0.3	11.4	0.56	0.0018	1.73	17.16	0.0079	153.68	45.26	0.1	0.18
41	Laloda	34.6	84.94	0.023	0.25	45.14	0.32	12.13	0.6	0.0019	1.84	18.26	0.0084	163.51	48.15	0.1	0.19
42	Magar	34.2	83.96	0.023	0.25	44.61	0.31	11.99	0.59	0.0019	1.82	18.05	0.0083	161.62	47.59	0.1	0.18
43	Matorda	30.1	73.9	0.02	0.22	39.27	0.28	10.55	0.52	0.0017	1.6	15.88	0.0073	142.24	41.89	0.09	0.16

44	Mehergarh Batta	31.5	77.33	0.021	0.23	41.09	0.29	11.04	0.54	0.0018	1.68	16.62	0.0077	148.86	43.84	0.09	0.17
45	Mehmudpur Jattan	31.21	76.62	0.021	0.23	40.71	0.29	10.94	0.54	0.0017	1.66	16.47	0.0076	147.49	43.43	0.09	0.17
46	Nardu	31.29	76.82	0.021	0.23	40.82	0.29	10.97	0.54	0.0017	1.67	16.51	0.0076	147.87	43.54	0.09	0.17
47	Nathu Majra	30.51	74.9	0.02	0.22	39.8	0.28	10.69	0.53	0.0017	1.62	16.1	0.0074	144.18	42.46	0.09	0.16
48	Paidan	61.1	150	0.041	0.45	79.71	0.56	21.41	1.05	0.0034	3.25	32.24	0.0149	288.74	85.03	0.18	0.33
49	Paror	32.4	79.54	0.022	0.24	42.27	0.3	11.35	0.56	0.0018	1.73	17.1	0.0079	153.11	45.09	0.09	0.17
50	Patran	33.68	82.69	0.022	0.25	43.94	0.31	11.8	0.58	0.0019	1.79	17.77	0.0082	159.16	46.87	0.1	0.18
51	Raipur	60.63	148.85	0.04	0.44	79.09	0.56	21.25	1.04	0.0034	3.23	32	0.0148	286.52	84.38	0.18	0.33
52	Raisal	34.2	83.96	0.023	0.25	44.61	0.31	11.99	0.59	0.0019	1.82	18.05	0.0083	161.62	47.59	0.1	0.18
53	Rasauli	46.86	115.04	0.031	0.34	61.13	0.43	16.42	0.81	0.0026	2.49	24.73	0.011	221.44	65.21	0.14	0.25
54	Rasulpur	59.3	14.58	0.039	0.43	77.36	0.54	20.78	1.02	0.0033	3.16	31.29	0.014	280.23	82.52	0.17	0.32
55	Rathian	72.93	179.05	0.048	0.53	95.14	0.67	25.56	1.26	0.0041	3.88	38.49	0.018	344.64	101.49	0.21	0.39
56	Shadipur	34.39	84.43	0.023	0.25	44.86	0.32	12.05	0.59	0.0019	1.83	18.15	0.0084	162.51	47.86	0.1	0.19
57	Salempur Sekhan	32.6	80.04	0.022	0.24	42.53	0.3	11.42	0.56	0.0018	1.74	17.2	0.008	154.06	45.37	0.09	0.18
58	Samaspur	31	76.11	0.021	0.23	40.44	0.29	10.86	0.53	0.0017	1.65	16.36	0.0076	146.49	43.14	0.09	0.17
59	Sanoulian	37.77	92.73	0.025	0.28	49.27	0.35	13.24	0.65	0.0021	2.01	19.93	0.009	178.49	52.56	0.11	0.2
60	Sarkara Farm	51.33	126.02	0.034	0.38	66.96	0.47	17.99	0.88	0.0028	2.73	27.09	0.0125	242.57	77.43	0.15	0.28
61	Seona	66.54	163.36	0.044	0.49	86.8	0.61	23.32	1.15	0.0037	3.54	35.12	0.016	314.44	92.6	0.19	0.36
62	Shahpur Radian	32.6	80.04	0.022	0.24	42.53	0.3	11.42	0.56	0.0018	1.74	17.2	0.008	154.06	45.37	0.09	0.18
63	Shankarpur	33.56	82.39	0.022	0.25	43.78	0.31	11.76	0.58	0.0019	1.79	17.71	0.008	158.59	46.7	0.1	0.18
64	Sheikhupur	34.2	83.96	0.023	0.25	44.61	0.31	11.99	0.59	0.0019	1.82	18.05	0.0083	161.62	47.59	0.1	0.18
65	Sirinagar	34.2	83.96	0.023	0.25	44.61	0.31	11.99	0.59	0.0019	1.82	18.05	0.0083	161.62	47.59	0.1	0.18
66	Thuha Patti	31.1	76.35	0.021	0.23	40.57	0.29	10.9	0.54	0.0017	1.66	16.41	0.0076	146.97	43.28	0.09	0.17
67	Thuhi	31.1	76.35	0.021	0.23	40.57	0.29	10.9	0.54	0.0017	1.66	16.41	0.0076	146.97	43.28	0.09	0.17
68	Todarwal	83.34	204.6	0.055	0.61	108.72	0.76	29.21	1.44	0.0046	4.44	43.98	0.0203	393.83	115.98	0.24	0.45

69	Uppli	38	93.29	0.025	0.28	49.57	0.35	13.32	0.65	0.0021	2.02	20.05	0.0093	179.57	52.88	0.11	0.2
70	Wazidpur	62.5	153.44	0.042	0.46	81.53	0.57	21.9	1.08	0.0035	3.33	32.98	0.0152	295.35	86.98	0.18	0.34

* Retention, + Concentrtion

Table 2: Radiological doses to different organs and tissues

Sr. No.	Adr-enals	BW\$	BS#	Brain	Breasts	St Wall	SI wall	ULI wall	LLI wall	Kidneys	Liver	Lungs	Muscle	Ovaries	Pancreas	RM@	Skin	Spleen	Testes	Thymus	Thyroid	Uterus	R^	E*
	μSv	μSv	μSv	μSv	μSv	μSv	μSv	μSv	μSv	μSv	μSv	μSv	μSv	μSv	μSv	μSv	μSv	μSv	μSv	μSv	μSv	μSv	μSv	μSv
1	20.12	20.12	579.86	20.12	20.12	23.54	28.31	71.63	174	208.07	78.45	20.12	20.12	20.12	20.12	61.4	20.12	20.12	19.78	20.12	20.12	20.12	22.17	44.34
2	20.12	20.12	579.86	20.12	20.12	23.54	28.31	71.63	174	208.07	78.45	20.12	20.12	20.12	20.12	61.4	20.12	20.12	19.78	20.12	20.12	20.12	22.17	44.34
3	2.49	2.49	71.67	2.49	2.49	2.91	3.5	8.85	21.5	25.72	9.7	2.49	2.49	2.49	2.49	7.59	2.49	2.49	2.45	2.49	2.49	2.49	2.74	5.48
4	5.56	5.56	160.19	5.56	5.56	6.5	7.82	19.79	48.06	57.48	21.67	5.56	5.56	5.56	5.56	16.96	5.56	5.56	5.47	5.56	5.56	5.56	6.12	12.25
5	2.92	2.92	84.2	2.92	2.92	3.42	4.11	10.4	25.26	30.21	11.39	2.92	2.92	2.92	2.92	8.92	2.92	2.92	2.87	2.92	2.92	2.92	3.22	6.44
6	2.96	2.96	85.35	2.96	2.96	3.46	4.17	10.54	25.6	30.63	11.55	2.96	2.96	2.96	2.96	9.04	2.96	2.96	2.91	2.96	2.96	2.96	3.26	6.53
7	2.96	2.96	85.35	2.96	2.96	3.46	4.17	10.54	25.6	30.63	11.55	2.96	2.96	2.96	2.96	9.04	2.96	2.96	2.91	2.96	2.96	2.96	3.26	6.53
8	2.27	2.27	65.37	2.27	2.27	2.65	3.19	8.08	19.61	23.46	8.84	2.27	2.27	2.27	2.27	6.92	2.27	2.27	2.23	2.27	2.27	2.27	2.5	5
9	2.83	2.83	81.55	2.83	2.83	3.31	3.98	10.07	24.46	29.26	11.03	2.83	2.83	2.83	2.83	8.63	2.83	2.83	2.78	2.83	2.83	2.83	3.12	6.24
10	5.71	5.71	164.62	5.71	5.71	6.68	8.04	20.34	49.39	59.07	22.27	5.71	5.71	5.71	5.71	17.43	5.71	5.71	5.62	5.71	5.71	5.71	6.29	12.59
11	2.34	2.34	67.32	2.34	2.34	2.73	3.29	8.32	20.2	24.16	9.11	2.34	2.34	2.34	2.34	7.13	2.34	2.34	2.3	2.34	2.34	2.34	2.57	5.15
12	3.83	3.83	110.22	3.83	3.83	4.47	5.38	13.61	33.06	39.55	14.91	3.83	3.83	3.83	3.83	11.67	3.83	3.83	3.76	3.83	3.83	3.83	4.21	8.43
13	6.61	6.61	190.59	6.61	6.61	7.74	9.31	23.54	57.18	68.39	25.79	6.61	6.61	6.61	6.61	20.18	6.61	6.61	6.5	6.61	6.61	6.61	7.29	14.57
14	2.28	2.28	65.59	2.28	2.28	2.66	3.2	8.1	19.68	23.53	8.87	2.28	2.28	2.28	2.28	6.94	2.28	2.28	2.24	2.28	2.28	2.28	2.51	5.02
15	9.62	9.62	277.12	9.62	9.62	11.25	13.53	34.23	83.13	99.44	37.49	9.62	9.62	9.62	9.62	29.34	9.62	9.62	9.45	9.62	9.62	9.62	10.6	21.19
16	6.25	6.25	180.11	6.25	6.25	7.31	8.79	22.25	54.03	64.63	24.37	6.25	6.25	6.25	6.25	19.07	6.25	6.25	6.14	6.25	6.25	6.25	6.89	13.77
17	4.71	4.71	135.73	4.71	4.71	5.51	6.63	16.77	40.72	48.7	18.36	4.71	4.71	4.71	4.71	14.37	4.71	4.71	4.63	4.71	4.71	4.71	5.19	10.38
18	3.18	3.18	91.65	3.18	3.18	3.72	4.47	11.32	27.49	32.89	12.4	3.18	3.18	3.18	3.18	9.7	3.18	3.18	3.13	3.18	3.18	3.18	3.5	7.01
19	2.34	2.34	67.54	2.34	2.34	2.74	3.3	8.34	20.26	24.24	9.14	2.34	2.34	2.34	2.34	7.15	2.34	2.34	2.3	2.34	2.34	2.34	2.58	5.16
20	5.05	5.05	145.59	5.05	5.05	5.91	7.11	17.99	43.68	52.24	19.7	5.05	5.05	5.05	5.05	15.42	5.05	5.05	4.97	5.05	5.05	5.05	5.57	11.13
21	2.46	2.46	70.95	2.46	2.46	2.88	3.46	8.76	21.29	25.46	9.6	2.46	2.46	2.46	2.46	7.51	2.46	2.46	2.42	2.46	2.46	2.46	2.71	5.43
22	2.29	2.29	66.02	2.29	2.29	2.68	3.22	8.16	19.81	23.69	8.93	2.29	2.29	2.29	2.29	6.99	2.29	2.29	2.25	2.29	2.29	2.29	2.52	5.05

© 2025 Author(s). This article is published under the CC-BY license at <http://jpr.vyomhansjournals.com>.

5.7. Urinary Bladder (UB)

The transit of uranium activity into the urinary bladder may transpire either through direct influx from the bloodstream or via the urinary pathway originating from the kidney. As per biokinetic model (Fig. 2), approximately 63% of uranium undergoes elimination from the body via urine, traversing through the urinary bladder compartment. The mean retention of uranium within the urinary bladder was determined to be 0.0128 μg , and ranged from 0.0073 to 0.0650 μg (Table 1). Fig. 7d demonstrates shorter period of time for uranium saturation in this organ.

5.8. Excretion from the body

Hair Biokinetic model includes an extra excretion site in addition to two previous sites, i.e., faeces and urine [21]. The maximum excretion occurs through faeces ranging from 41.89 $\mu\text{g d}^{-1}$ to 371.57 $\mu\text{g d}^{-1}$, followed by hair (0.16 $\mu\text{g d}^{-1}$ to 1.44 $\mu\text{g d}^{-1}$), and then urine (0.09 $\mu\text{g d}^{-1}$ to 0.78 $\mu\text{g d}^{-1}$) as illustrated in spatial distribution maps (Fig. 8) and Table 1. The median daily excretion ratio of uranium in urine and in hair, measured in the individuals who ingested more than 10 $\mu\text{g d}^{-1}$ of uranium in drinking water, was estimated to be 0.67 [44]. The detailed interpretation of this ratio (0.67) is given by Li et al. [21]. In the present study using Hair Biokinetic model of uranium, a compartment for nails is not incorporated in Fig. 2, due to the lower concentration of uranium in nails compared to the concentrations in urine and in hair. However, uranium excretion in nails can be estimated by the ratio of uranium excretion rate of 0.014 in nails and in hair [21].

5.9. Radiological Doses to Organs and Tissues

Radionuclides, including uranium, with a long biological half-life are dangerous at very low doses. The radiological effects of natural uranium are low compared with its chemical toxicity. But these effects cannot be ignored if insoluble uranium compounds remain in the body for a longer period. The doses delivered to different body organs and other tissues can be calculated according to dose conversion factors provided by the ICRP [45]. Upon entry into the human

body, uranium exerts deleterious effects, with an average effective dose of 8.71 μSv recorded in the study area. The gastrointestinal tract (GIT) compartments experience varying impacts, with the stomach, small intestine, lower large intestine, and upper large intestine receiving average doses of 4.62 μSv , 5.56 μSv , 14.06 μSv , and 34.16 μSv , respectively (Table 2).

Additionally, Table 2 delineates the calculated doses for other organs and tissues, revealing elevated average doses of 113.85 μSv and 40.85 μSv for bone surfaces and kidney sites, respectively. Other soft tissues in the study area, encompassing adrenals, brain, breasts, lungs, muscle, ovaries, pancreas, skin, spleen, thymus, and uterus, exhibit average doses ranging from 2.27 to 20.12 μSv , with a mean value of 3.95 μSv . Furthermore, the liver receives a comparatively higher dose than several other internal organs and tissues, ranging from 8.84 μSv to 78.45 μSv in the studied area, with an average of 15.40 μSv . Fig. 9 depicts the distribution of dose to various organs and tissues in the human body which shows that the percentage of dose to bone surfaces is highest at 38.5%, followed by kidneys (13.8%), LLI walls (11.5%), Liver (5.2%), ULI walls (4.8%), Red marrow (4.1%), SI wall (1.9%), St wall (1.6%) and all other organs and tissues with 1.3% each. These elevated dosage levels present in the human body at the specific location under investigation pose a significant risk to the organs and sensitive tissues, as they are exposed to both the radiological and chemical toxicity of uranium.

6. Conclusions

Li's Hair Compartment Biokinetic Model has advantages over the ICRP Biokinetic Model. As a consequence, it has been used to investigate empirically the uranium retention, excretion and radiological dose delivered to human body organs and tissues due to ingestion of uranium from the groundwater of Patiala district. The average concentration of uranium in water sources of the studied area has been found to be 52.42 $\mu\text{g L}^{-1}$ (30.10 to 267 $\mu\text{g L}^{-1}$). The data obtained from the analysis indicated that all the recorded values are above the WHO recommended limits (30 $\mu\text{g L}^{-1}$) [46]. Furthermore, about 26% of the samples surpassed the

limit set by AERB ($60 \mu\text{g L}^{-1}$) [47]. It has been found from the time-dependent studies of uranium that the vital organs targeted by natural uranium through the ingestion route are the kidneys, liver, other soft tissues and cortical bone volume and were not saturated even after a span of 60 years. Excretion rate of uranium from hair is higher than the urine which justifies the use of Li's model. The radiological dose delivered to body organs and tissues through the ingestion route is not uniform. The highest percentage of dose is delivered to bone surfaces (38.5%), followed by kidneys (13.8%), LLI walls (11.5%), Liver (5.2%), ULI walls (4.8%), Red marrow (4.1%), and other organs and tissues (1.3%). Furthermore, the overall uranium distribution in Punjab province schematically demonstrates the higher values in the southern Punjab regions (Fig. 10). Fig. 10 was constructed based on previous studies, incorporating data from 70 locations within the Patiala district, resulting in improved spatial mapping compared to the remainder of the map. A comprehensive analysis of spatial distribution warrants future investigation, with heightened emphasis on collecting maximum samples from diverse districts within Punjab. This study also emphasizes the continuous need for vigilance and measures to mitigate the potential adverse effects of uranium on human health. It is evident that urgent action is required to address this pressing issue and safeguard the well-being of the inhabitants of Patiala district.

Acknowledgements: Author acknowledges the help of Pargin Bangotra and Bhawna Sehrawat, faculty of the Department of Physics, Netaji Subhas University of Technology, Dwarka-110078, New Delhi, India for their help in analysis of data and drawing of figures. Dr Satnam Singh of Baba Bhag Singh University, Jalandhar, Punjab helped in preparing LATEX file of paper. He also deserves my appreciation and gratitude.

Authorship contribution: It is a single author paper and there is no contribution of other authors in this study.

Funding: No funding has been received from outside agencies.

Conflict of interest: Author has no conflict of interest with anyone.

Declaration: It is an original data and has neither been sent elsewhere nor published anywhere in this format.

Similarity Index: I hereby confirm that there is no similarity index in abstract and conclusion while overall is less than 10% where individual source contribution is 2% or less than it.

References

- [1] UNESCO. (2022). Groundwater: Making the invisible visible (The United Nations World Water Development Report 2022). Paris: UNESCO.
- [2] Bangotra, P., Jakhu, R., Prasad, M., Aswal, R. S., Ashish, A., Mushtaq, Z., & Mehra, R. (2023). Investigation of heavy metal contamination and associated health risks in groundwater sources of southwestern Punjab, India. *Environmental Monitoring and Assessment*, 195(3), 367. <https://doi.org/10.1007/s10661-023-10959-7>
- [3] Hu, Q.-H., Weng, J.-Q., & Wang, J.-S. (2010). Sources of anthropogenic radionuclides in the environment: A review. *Journal of Environmental Radioactivity*, 101(6), 426–437. <https://doi.org/10.1016/j.jenvrad.2008.08.004>
- [4] Prasad, M., Aswal, R. S., Shrivastava, U., Joshi, A., Panwar, P., Bangotra, P., & Ramola, R. C. (2024). Levels and effects of uranium in groundwater sources of Shivalik hills, outer Himalaya, India. *Journal of Radioanalytical and Nuclear Chemistry*, 333(5), 2495–2504. <https://doi.org/10.1007/s10967-023-08906-4>
- [5] Stalder, E., Blanc, A., Haldimann, M., & Dudler, V. (2012). Occurrence of uranium in Swiss drinking water. *Chemosphere*, 86(6), 672–679. <https://doi.org/10.1016/j.chemosphere.2011.11.022>
- [6] Gainon, F., Surbeck, H., & Zwahlen, F. (2007). Natural radionuclides in groundwater as pollutants and as useful tracer. In T. D. Bullen (Ed.), *Water-rock Interaction* (Vol. 53). <https://doi.org/10.1201/NOE0415451369.ch154>
- [7] Giri, S., Singh, G., & Jha, V. N. (2011). Evaluation of radionuclides in groundwater around proposed uranium mining sites in Bagjata and Banduhurang, Jharkhand (India). *Radioprotection*, 46(1), 39–57. <https://doi.org/10.1051/radiopro/2010056>
- [8] Ioannidou, A., Samaropoulos, I., Efstathiou, M., & Pashalidis, I. (2011). Uranium in ground water samples of Northern Greece. *Journal of Radioanalytical and Nuclear Chemistry*, 289(2), 551–555. <https://doi.org/10.1051/epjconf/20122403005>
- [9] Virk, H. S. (2017). A crisis situation due to uranium and heavy metal contamination of ground waters

- in Punjab state, India: A preliminary report. *Research and Reviews: Journal of Toxicology*, 7(2), 6–11. <https://medicaljournals.stmjournals.in/..article/view/3>
- [10] Sahoo, S. K., Jha, S. K., Jha, V. N., Patra, A. C., & Kulkarni, M. S. (2021). Survey of uranium in drinking water sources in India. *Current Science*, 120(9), 1482–1490. <https://doi.org/10.18520/cs/v120/i9/1482-1490>
- [11] Sahoo, P. K., Virk, H. S., Powell, M. A., Kumar, R., Pattanaik, J. K., Salomão, G. N., Mittal, S., Chouhan, L., Nandabalan, Y. K., & Tiwari, R. P. (2022). Meta-analysis of uranium contamination in groundwater of the alluvial plains of Punjab, northwest India: Status, health risk, and hydrogeochemical processes. *Science of the Total Environment*, 807, 151753. <https://doi.org/10.1016/j.scitotenv.2021.151753>
- [12] Mehra, R., Bangotra, P., & Kaur, K. (2015). ²²²Rn and ²²⁰Rn levels of Mansa and Muktsar district of Punjab, India. *Frontiers in Environmental Science*, 3, 37. <https://doi.org/10.3389/fenvs.2015.00037>
- [13] Jakhu, R., Mehra, R., & Bangotra, P. (2020). Risk assessment of ²²⁶Ra and ²²²Rn from the drinking water in the Jalandhar and Kapurthla districts of Punjab. *SN Applied Sciences*, 2(6), 1032. <https://doi.org/10.1007/s42452-020-2833-x>
- [14] World Health Organization. (2005). *Uranium in drinking-water: Background document for development of WHO guidelines for drinking-water quality*. Geneva: World Health Organization.
- [15] Kayzar, T. M., Villa, A. C., Lobaugh, M. L., Gaffney, A. M., & Williams, R. W. (2014). Investigating uranium distribution in surface sediments and waters: A case study of contamination from the Juniper Uranium Mine, Stanislaus National Forest, CA. *Journal of Environmental Radioactivity*, 136, 85–97. <https://doi.org/10.1016/j.jenvrad.2014.04.018>
- [16] Chen, S. B., Zhu, Y. G., & Hu, Q. H. (2005). Soil to plant transfer of ²³⁸U, ²²⁶Ra and ²³²Th on a uranium mining-impacted soil from southeastern China. *Journal of Environmental Radioactivity*, 82(2), 223–236. <https://doi.org/10.1016/j.jenvrad.2005.01.009>
- [17] Bangotra, P., Sharma, M., Mehra, R., Jakhu, R., Singh, A., Gautam, A. S., & Gautam, S. (2021). A systematic study of uranium retention in human organs and quantification of radiological and chemical doses from uranium ingestion. *Environmental Technology & Innovation*, 21, 101360. <https://doi.org/10.1016/j.eti.2021.101360>
- [18] Li, W. B., Roth, P., Wahl, W., Oeh, U., Höllriegl, V., & Paretzke, H. G. (2005). Biokinetic modeling of uranium in man after injection and ingestion. *Radiation and Environmental Biophysics*, 44(1), 29–40. <https://doi.org/10.1007/s00411-005-0272-0>
- [19] Zamora, M. L., Tracy, B. L., Zielinski, J. M., Meyerhof, D. P., & Moss, M. A. (1998). Chronic ingestion of uranium in drinking water: A study of kidney bioeffects in humans. *Toxicological Sciences*, 43(1), 68–77. <https://doi.org/10.1006/toxs.1998.2426A>
- [20] Kurttio, P., Auvinen, A., Salonen, L., Saha, H., Pekkanen, J., Mäkeläinen, I., Väisänen, S. B., Penttilä, I. M., & Komulainen, H. (2002). Renal effects of uranium in drinking water. *Environmental Health Perspectives*, 110(4), 337–342. <https://doi.org/10.1289/ehp.02110337>
- [21] Li, W. B., Karpas, Z., Salonen, L., Kurttio, P., Muikku, M., Wahl, W., Höllriegl, V., Hoeschen, C., & Oeh, U. (2009). A compartmental model of uranium in human hair for protracted ingestion of natural uranium in drinking water. *Health Physics*, 96(6), 636–645. <https://doi.org/10.1097/01.HP.000345023.46165.1c>
- [22] Shrivastava, B. K. (2015). Elevated uranium and toxic elements concentration in groundwater in Punjab state of India: Extent of the problem and risk due to consumption of unsafe drinking water. *Water Quality, Exposure and Health*, 7(3), 407–421. <https://doi.org/10.1007/s12403-014-0144-4>
- [23] Government of India, Northwestern Region, Chandigarh. (2013). *Central Ground Water Board (CGWB), Patiala District, Punjab. Ministry of Water Resources*. Chandigarh: Government of India.
- [24] Virk, H. S. (2022). Groundwater contamination in Punjab due to high levels of nitrate (NO₃⁻) and its health hazards: A preliminary report. *Journal of Toxicology*, 12(3), 18–26.
- [25] Nizam, S., Virk, H. S., & Sen, I. S. (2022). High levels of fluoride in groundwater from Northern parts of Indo-Gangetic plains reveals detrimental fluorosis health risks. *Environmental Advances*, 8, 100200. <https://doi.org/10.1016/j.envadv.2022.100200>
- [26] Virk, H. S. (2023). A study of groundwater contamination of Patiala district as a ‘hot spot’ in Punjab. *Journal of Water Pollution & Purification Research*, 10(1), 1–13.
- [27] World Bank. (2020, January). *Toward managing rural drinking water quality in the state of Punjab, India* (Water Global Practice Discussion Paper No. W19002). Washington, DC: World Bank; Water Global Practice. <https://documents1.worldbank.org/.../Punjab-India.pdf>
- [28] Virk, H. S. (2019). Uranium content anomalies in groundwater of Patiala District of Punjab (India) for the assessment of excess cancer risk. *Research & Reviews: Journal of Oncology and Hematology*, 8(2), 13–19.
- [29] Virk, H. S. (2023). A critical evaluation of mercury contamination in groundwater of Punjab. *Journal of Water Pollution & Purification Research*, 10(3), 1–11. STM Journals. Available online since April 2, 2024. <https://techjournals.stmjournals.in/.../1535>
- [30] Breustedt, B., Giussani, A., & Noßke, D. (2018). Internal dose assessments—Concepts, models and uncertainties. *Radiation Measurements*, 115, 49–54. <https://doi.org/10.1016/j.radmeas.2018.06.013>
- [31] Leggett, R. W., & Harrison, J. D. (1995). Fractional absorption of ingested uranium in humans. *Health Physics*, 68(4), 484–498.

- <https://doi.org/10.1097/00004032-199504000-00005>
- [32] Bassett, S. H., Frankel, A., Cedars, N., VanAlstine, H., Waterhouse, C., & Cusson, K. (1948). The excretion of hexavalent uranium following intravenous administration. II, Studies on human subjects. Rochester, NY: University of Rochester, Atomic Energy Project.
- [33] Bernard, S. R., & Struxness, E. G. (1957). A study of the distribution and excretion of uranium in man: An interim report. Oak Ridge, TN: Oak Ridge National Laboratory.
- [34] Li, W. B., Salonen, L., Muikku, M., Wahl, W., Höllriegl, V., Oeh, U., Roth, P., & Rahola, T. (2006). Internal dose assessment of natural uranium from drinking water based on biokinetic modeling and individual bioassay monitoring: A study of a Finnish family. *Health Physics*, 90(6), 533–543. <https://doi.org/10.1097/01.HP.0000184671.58054.3c>
- [35] Terepka, A. R., Toribara, T. Y., & Neuman, W. F. (1964). Skeletal retention of uranium in man. In *Proceedings of the 46th Meeting of the Endocrinology Society* (Vol. 29, p. 76).
- [36] International Commission on Radiological Protection (ICRP). (2015). Occupational intakes of radionuclides: Part 1. *Annals of the ICRP*, 44.
- [37] International Commission on Radiological Protection (ICRP). (2017). Occupational intakes of radionuclides: Part 3. *Annals of the ICRP*, 46(3–4), 1–486.
- [38] Bangotra, P., Mehra, R., Jakhu, R., Pandit, P., & Prasad, M. (2019). Quantification of an alpha flux based radiological dose from seasonal exposure to ²²²Rn, ²²⁰Rn and their different EEC species. *Scientific Reports*, 9(1), 2515. <https://doi.org/10.1038/s41598-019-38871-6>
- [39] Pandit, P., Mangala, P., Saini, A., Bangotra, P., Kumar, V., Mehra, R., & Ghosh, D. (2020). Radiological and pollution risk assessments of terrestrial radionuclides and heavy metals in a mineralized zone of the Siwalik region (India). *Chemosphere*, 254, 126857. <https://doi.org/10.1016/j.chemosphere.2020.126857>
- [40] Hakeem, Z., Bangotra, P., Gautam, A. S., Sharma, M., Suman, Gautam, S., Singh, K., Kumar, Y., & Jain, P. (2024). Satellite or ground-based measurements for air pollutants (PM_{2.5}, PM₁₀, SO₂, NO₂, O₃) data and their health hazards: Which is most accurate and why? *Environmental Monitoring and Assessment*, 196(4), 342. <https://doi.org/10.1007/s10661-024-12462-z>
- [41] Fisenne, I. M., & Perry, P. M. (1985). Isotopic U concentration in human blood from New York City donors. *Health Physics*, 49(6), 1272–1275.
- [42] Moss, M. A., McCurdy, R. F., Dooley, K. C., Givner, M. L., Dymond, L. C., Slayter, J. M., & Courneya, M. M. (1983). Uranium in drinking water—Report on clinical studies in Nova Scotia. In *Chemical Toxicology and Clinical Chemistry of Metals: Proceedings of the 2nd International Conference* (pp. 149–152). Montreal, Canada.
- [43] Leggett, R. W. (1994). Basis for the ICRP's age-specific biokinetic model for uranium. *Health Physics*, 67(6), 589–610. <https://doi.org/10.1097/00004032-199412000-00002>
- [44] Karpas, Z., Paz-Tal, O., Lorber, A., Salonen, L., Komulainen, H., Auvinen, A., Saha, H., & Kurttio, P. (2005). Urine, hair, and nails as indicators for ingestion of uranium in drinking water. *Health Physics*, 88(3), 229–242. <https://doi.org/10.1097/01.hp.0000149883.69107.ab>
- [45] International Commission on Radiological Protection (ICRP). (1995). Age-dependent doses to members of the public from intake of radionuclides: Part 5. Compilation of ingestion and inhalation coefficients, ICRP, Publication 72. *Annals of the ICRP*, 26(1).
- [46] World Health Organization. (2012). *Uranium in drinking-water: Background document for development of WHO guidelines for drinking-water quality* (WHO/SDE/WSH/03.04/118). Geneva: World Health Organization. <https://www.who.int/.../uranium-background-document.pdf>
- [47] Atomic Energy Regulatory Board. (2004). Department of Atomic Energy (AERB). *Drinking water specification in India*. Delhi: Government of India.

Copyright and License

[© 2025 Hardev Singh Virk] This is an Open Access article published in "Graduate Journal of Interdisciplinary Research, Reports & Reviews" (Grad.J.InteR³), a **Diamond Open Access Journal** by **Vyom Hans Publications**. It is published with a Creative Commons Attribution - CC-BY4.0 International License. This license permits unrestricted use, distribution, and reproduction in any medium, provided the original author and source are credited.

How to Cite?

Hardev Singh Virk (2025). Assessment of Uranium Biokinetics and Organ Dose Estimation Following Ingestion from Groundwater in the Patiala District, Punjab, India. *Graduate Journal of Interdisciplinary Research, Reports and Reviews*, 3(02), 68–88. Retrieved from <https://jpr.vyomhansjournals.com/index.php/gjir/./view/58>